Allogeneic mesenchymal stem cells restore cardiac function in chronic ischemic cardiomyopathy via trilineage differentiating capacity

Henry C. Quevedo[a], Konstantinos E. Hatzistergos[a], Behzad N. Oskouei[a], Gary S. Feigenbaum[a], Jose E. Rodriguez[a], David Valdes[a], Pradip M. Pattany[a], Juan P. Zambrano[a,b], Qinghua Hu[a], Ian McNiece[a,b], Alan W. Heldman[a,b], and Joshua M. Hare[a,b,1]

[a]Interdisciplinary Stem Cell Institute and [b]Department of Medicine, Cardiovascular Division, Miller School of Medicine, University of Miami, Miami, FL 33136

Edited by Eugene Braunwald, Brigham and Women's Hospital, Boston, MA, and approved June 30, 2009 (received for review March 23, 2009)

The mechanism(s) underlying cardiac reparative effects of bone marrow-derived mesenchymal stem cells (MSC) remain highly controversial. Here we tested the hypothesis that MSCs regenerate chronically infarcted myocardium through mechanisms comprising long-term engraftment and trilineage differentiation. Twelve weeks after myocardial infarction, female swine received catheter-based transendocardial injections of either placebo ($n = 4$) or male allogeneic MSCs (200 million; $n = 6$). Animals underwent serial cardiac magnetic resonance imaging, and in vivo cell fate was determined by co-localization of Y-chromosome (Y^{pos}) cells with markers of cardiac, vascular muscle, and endothelial lineages. MSCs engrafted in infarct and border zones and differentiated into cardiomyocytes as ascertained by co-localization with GATA-4, Nkx2.5, and α-sarcomeric actin. In addition, Y^{pos} MSCs exhibited vascular smooth muscle and endothelial cell differentiation, contributing to large and small vessel formation. Infarct size was reduced from 19.3 ± 1.7% to 13.9 ± 2.0% ($P < 0.001$), and ejection fraction (EF) increased from 35.0 ± 1.7% to 41.3 ± 2.7% ($P < 0.05$) in MSC but not placebo pigs over 12 weeks. This was accompanied by increases in regional contractility and myocardial blood flow (MBF), particularly in the infarct border zone. Importantly, MSC engraftment correlated with functional recovery in contractility ($R = 0.85$, $P < 0.05$) and MBF ($R = 0.76$, $P < 0.01$). Together these findings demonstrate long-term MSC survival, engraftment, and trilineage differentiation following transplantation into chronically scarred myocardium. MSCs are an adult stem cell with the capacity for cardiomyogenesis and vasculogenesis which contribute, at least in part, to their ability to repair chronically scarred myocardium.

cardiac chimerism | cellular cardiomyoplasty | heart failure | catheter delivery

The past decade has witnessed increasing development of cell-based therapeutics for cardiac disorders (1), with lead candidates being autologous whole bone marrow (2, 3) and mesenchymal stem cells (4, 5), which are available from a variety of tissue sources. A major impediment to the advancement of this field is that mechanistic understanding substantially lags clinical observations (6). In this regard, it remains highly controversial whether cell-based therapies improve cardiac function by engraftment and differentiation (cell autonomous effects) (6–8) or by releasing paracrine factors (a cell nonautonomous effect) (9–13). Mesenchymal stem cells (MSCs) are a particularly attractive therapeutic candidate, having the capacity for immunoprivilege and multilineage differentiation (14, 15), and there are ongoing trials of this cell type as both autologous and allogeneic grafts (16). Although the potential of MSCs to adopt cardiac phenotypes has been shown in vitro (14, 17, 18), several recent studies question the potential of in vivo differentiation, with low rates of cell survival and engraftment being the suggested causes (19–22).

To address this important controversy, we tested the hypothesis that allogeneic MSCs possess the ability to engraft and differentiate in chronically infarcted myocardium. Moreover, we correlated cell engraftment with measures of functional recovery using cardiac magnetic resonance imaging (MRI). Employing both BrdU labeled and sex-mismatched MSCs in a miniswine model of chronic ischemic cardiomyopathy, we sought to demonstrate the in vivo tri-lineage potential of allogeneic MSCs.

Results

MSCs Retention and Engraftment. Male MSCs (2.0×10^8 cells) or vehicle were injected into adult female miniswine with chronically scarred myocardial infarctions (MI), and animals were killed 3 months later. MSC engraftment was identified using both BrdU ($BrdU^{pos}$, Fig. 1 *A–C*) and the Y-chromosome (Y^{pos}) (Fig. 2 *A–F*). Importantly, appropriate negative controls, including female MI nontreated hearts, confirmed the specificity of the porcine Y-chromosome for the fluorescence in situ hybridization (FISH) analysis (see Fig. S1 *b–c* and *e–f*). MSCs were detected only in infarct (15.0 ± 2 .0 cells/100 mm^2) and infarct border (17.0 ± 6.2 cells/100 mm^2) zones of MSC-treated animals (Fig. 2*H*), representing 4.1% of the cardiomyocyte nuclei in the peri-ischemic area. A total of 17,854 cardiomyocytes were evaluated from the infarct and border zone of MSC-treated hearts (3,570 ± 444 cardiomyocytes per animal, $n = 6$ for MSC-treated group, $n = 4$ for placebo, respectively). The number of $BrdU^{pos}$ cells was ≈3-fold greater than the Y^{pos} cells. Despite this, the percent of $BrdU^{pos}$ cells with evidence of differentiation was similar to that determined using Y-chromosome FISH (Fig. S2).

Cardiac Differentiation. Of engrafted Y^{pos} cells, 14.0% ± 4.0% exhibited evidence of myocyte commitment (5.5×10^2 Y^{pos} myocytes per 10^6 cardiomyocyte nuclei), based upon co-staining with cardiac transcription factors (GATA-4 and Nkx2.5) or structural cardiac proteins (α-sarcomeric actinin and tropomyosin; Fig. 2 *C–H*). Importantly, differentiated myocytes showed evidence of coupling to host myocardium via connexin-43 (Fig. 2*E*). Newly-formed Y^{pos} myocytes in the border ischemic area had a diameter of 15.4 ± 0.6 μm, which was similar to other myocytes in the MSC-treated hearts (15.4 ± 0.3 μm), but smaller than those in placebo hearts (20.4 ± 0.5 μm, $P < 0.01$; Fig. S3).

Author contributions: B.N.O., Q.H., and J.M.H. designed research; H.C.Q., K.E.H., B.N.O., G.S.F., P.M.P., J.E.R., D.V., J.P.Z., Q.H., I.M., and A.W.H. performed research; K.E.H., G.S.F., J.E.R., and P.M.P. contributed new reagents/analytic tools; H.C.Q., G.S.F., and J.M.H. analyzed data; and H.C.Q., K.E.H., G.S.F., and J.M.H. wrote the paper.

The authors declare no conflict of interest.

This article is a PNAS Direct Submission.

[1]To whom correspondence should be addressed. E-mail: jhare@med.miami.edu.

This article contains supporting information online at www.pnas.org/cgi/content/full/0903201106/DCSupplemental.

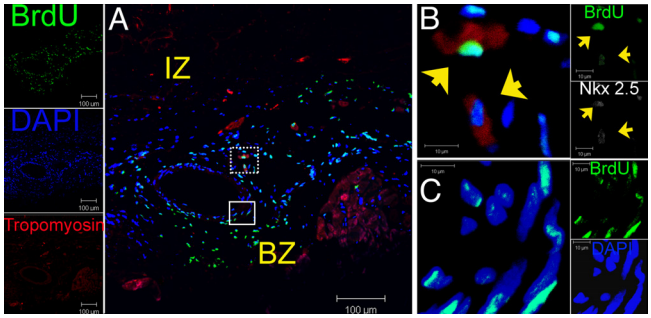

Fig. 1. Survival and distribution of transplanted MSCs in treated hearts. (*A*) Low power image of the infarct border region of MSC-treated heart depicting a band composing of BrdU^{pos} cells (green) 12 weeks posttransplantation forming a medium-size vessel composed of BrdU ^{pos} cells throughout the vascular wall. (*B*) High magnification of the dotted square in (*A*) illustrating two BrdU^{pos} nuclei (arrowheads) adjacent to the vessel, co-localized with cardiac transcription factor Nkx2.5 (white) and the structural protein tropomyosin (red) as depicted in the contiguous individual fluorescence channels on the right. (*C*) High power view of the square in (*A*) showing that BrdU^{pos} cells are distributed throughout the vessel wall. Individual fluorescence channels for Nkx2.5, BrdU, and DAPI are shown in the adjacent insets. For double immunofluorescence co-localizations, $n = 4$ for both MSC and placebo hearts. At least four tissue sections from infarct, border, and remote zone were evaluated per heart. IZ, infarct zone; BZ, border zone.

Vasculogenesis. MSCs participated in the formation of coronary vasculature as identified by co-staining with vascular muscle proteins (smooth muscle actinin, calponin, smooth muscle protein 22-α) and endothelial cell surface marker (factor VIII-related antigen/VWF; Fig. 3). A total of 744 vessels were evaluated from the injured areas of MSC-treated hearts (149 ± 35 vessels per animal, $n = 5$). Of these vessels, 3.4% contained significant numbers of Y^{pos} cells. Of the engrafted MSCs, 5.9 ± 1.8% exhibited a vascular smooth muscle cell phenotype, and 3.9 ± 3.0% formed endothelial cells. In the border zone, MSCs incorporated in both large and medium sized vessels (500 μm to 1 mm), contributing to both endothelial and smooth muscle layers (Fig. 3 *A–D*). In contrast, within the infarct zone, most of the new vessels had diameters <20 μm and were composed of single endothelial layers with no smooth muscle layers (Fig. 3 *D–E* and Fig. S1 *d–f*), consistent with capillary formation.

Nondifferentiated MSCs. Additional clusters of Y^{pos} cells (76.1 ± 4.9% of engrafted cell population) were located within the interstitial compartment. These cells had diameters of 8.1 ± 0.5 μm, smaller than myocytes, indicating an immature phase. These cells did not co-localize with markers of hematopoietic cell lineage (CD 45^{neg}, CD 68^{neg}) or have a cardiogenic phenotype (Fig. 3*F*).

Infarct Evolution. Cardiac MRI images documented a decrement in ejection fraction, transmural extension of myocardial scar, and left ventricular (LV) remodeling 12 weeks after anterior MI (Table 1). We next determined the impact of cell therapy on infarct size, measured as a percentage of the LV and as absolute volume of scar tissue. Using both of these parameters, infarct size was reduced by MSC therapy, resulting in a 29.0 ± 5.1% reduction in infarct size

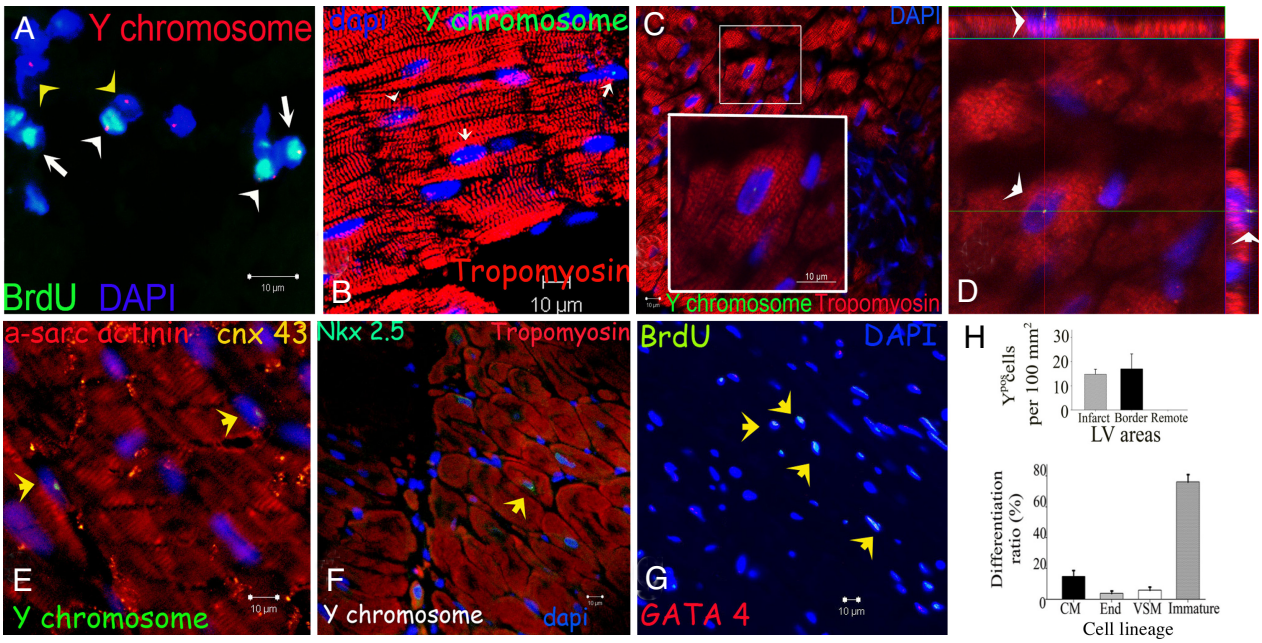

Fig. 2. Cardiogenic potential of transplanted MSCs. (*A*) Cluster of Y^{pos}/BrdU^{pos} cells (white arrowheads) located in infarct and border zones of treated hearts 12 weeks after MSCs implantation. Some of the transplanted MSCs do not exhibit BrdU^{pos} signal (green), but maintain Y^{pos} signal (red, yellow arrowheads). Conversely, another group shows BrdU^{pos} signal (white arrows) and negative Y chromosome signal due technique sensitivity. (*B*) Cluster of Y^{pos} cells (green, white arrows) in the border zone of MSC-treated animals co-localizing with tropomyosin (red). (*C*) Evidence of cardiac differentiation in a panoramic view of an infarct border zone of MSC-treated hearts. The inset depicts one Y^{pos} (green) myocyte co-stained with tropomyosin. High magnification of the square is shown in the inset. (*D*) Confocal microscopy analysis of the same cell by orthogonal section of a z-stack (arrows point the cell analyzed in xy-plane). (*E*) Two transplanted Y^{pos} cells (green, arrows) coupled with the resident cardiomyocytes by expressing connexin-43 (orange). (*F*) Evidence of cardiac commitment in the transplanted cell by the co-localization of Y^{pos} signal with the cardiac transcription factor Nkx2.5 (green, arrow). Nuclei were counterstained with DAPI in all of the immunofluorescence assays. (*G*) Cluster of BrdU^{pos} cells (green) in the border zone of MSC-treated animals exhibiting co-localization with transcription factor GATA-4 (red, arrows). (*H*) Quantitation of transplanted cells according to Y chromosome cell tracking. Y^{pos} cells show no preference in distribution according to LV areas (top). Importantly, at 12 weeks posttransplantation, implanted MSCs showed commitment to repopulate the three major cardiac cell lineages and maintain a reservoir of nondifferentiated cells (bottom). Cell quantification per unit area for the Y chromosome ($n = 6$ for MSC-treated hearts, $n = 4$ for placebo-treated hearts). At least four tissue sections for infarct, border, and remote zone per heart were evaluated. Total area evaluated 2,673.34 mm^2. CM, cardiomyocyte; End, endothelial cells; VSM, vascular smooth muscle.

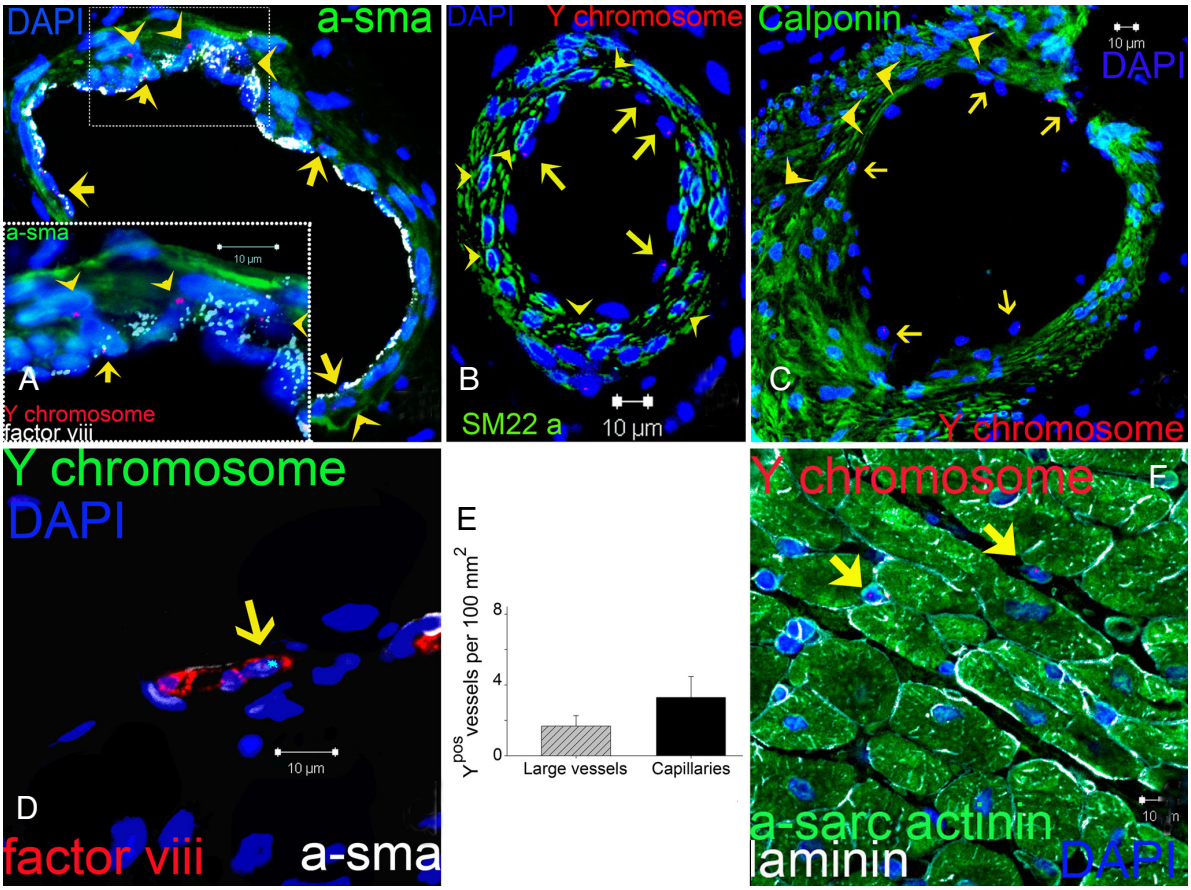

Fig. 3. Vascular differentiation of transplanted MSCs. (*A*) Representative image of a vessel containing numerous Y^{pos} cells co-localized with smooth muscle actinin (a-sma in green, arrowheads) and endothelial cells (factor VIII-related antigen in white, arrows). High magnification of the inset to visualize the Y^{pos} cells that co-localize with sma (arrowheads) and factor VIII-related antigen (white, arrows) demonstrating vascular smooth muscle and endothelial commitment, respectively. (*B* and *C*) Confirmation of Y^{pos} cells commitment into vascular structures as depicted by co-localization with SM22-α (*B*) and calponin (*C*, arrowheads in both pictures). Y^{pos} cells also commit to endothelial cell lineages (arrows). (*D*) Capillary formation with the incorporation of Y^{pos} cell (arrow) co-stained with factor VIII-related antigen depicting the luminal surface of the vessel. (*E*) Assessment of vessel number per unit area according to their respectively size. (*F*) Y^{pos} cells also reside in the interstitial compartment (arrows) of border myocardium in a nondifferentiated stage ($n = 6$ for MSC-treated hearts, $n = 4$ for placebo). At least 4 tissue sections from infarct, border, and remote zone were evaluated per animal.

[$P < 0.001$ by analysis of variance (ANOVA)]. Posthoc analysis revealed that infarct size reduction occurred by 8 weeks after therapy (Fig. 4*A–C*). In contrast, scar size remained constant in the placebo group ($P < 0.001$ vs. MSC; Table 1 and Fig. 4*C*). To address reverse remodeling, we quantified the decrease in the circumferential extent of the infarct scar. While the infarct region expanded 0.2 ± 1.4% in the placebo group at week 24, it was reduced by 14.1 ± 2.3% in the MSC-treated group ($P < 0.001$ by ANOVA; Table 1 and Fig. S4*b*). This effect was mirrored in the infarct region wall thickness, where there was continued thinning in the placebo

Table 1. Myocardial Infarct Phenotype before and 12 weeks after treatment

Parameter	Groups	Week 12	Week 24	*P*
MI Size, %LV mass	Placebo	19.6 ± 1.5	20.6 ± 1.1	0.76
	MSC	19.3 ± 1.7	13.9 ± 2.0	<0.001*†
Infarct volume, mL	Placebo	7.1 ± 0.4	8.0 ± 0.4	0.06
	MSC	7.4 ± 1.2	5.4 ± 1.1	<0.001†
LV mass, g	Placebo	36.5 ± 1.9	39.0 ± 0.6	0.75
	MSC	37.1 ± 3.2	37.5 ± 2.6	0.58
Circumferential extent of MI, % LV	Placebo	40.1 ± 2.8	40.3 ± 2.8	0.73
	MSC	42.1 ± 2.1	28.0 ± 2.8	<0.001*†
Wall thickness infarct, mm	Placebo	4.0 ± 0.1	3.6 ± 0.2	0.12
	MSC	3.9 ± 0.2	4.9 ± 0.4	0.049*†
Wall thickness remote, mm	Placebo	7.1 ± 0.5	7.4 ± 0.5	0.69
	MSC	6.6 ± 0.5	6.9 ± 0.3	0.62

*ANOVA between groups.
†ANOVA within groups.

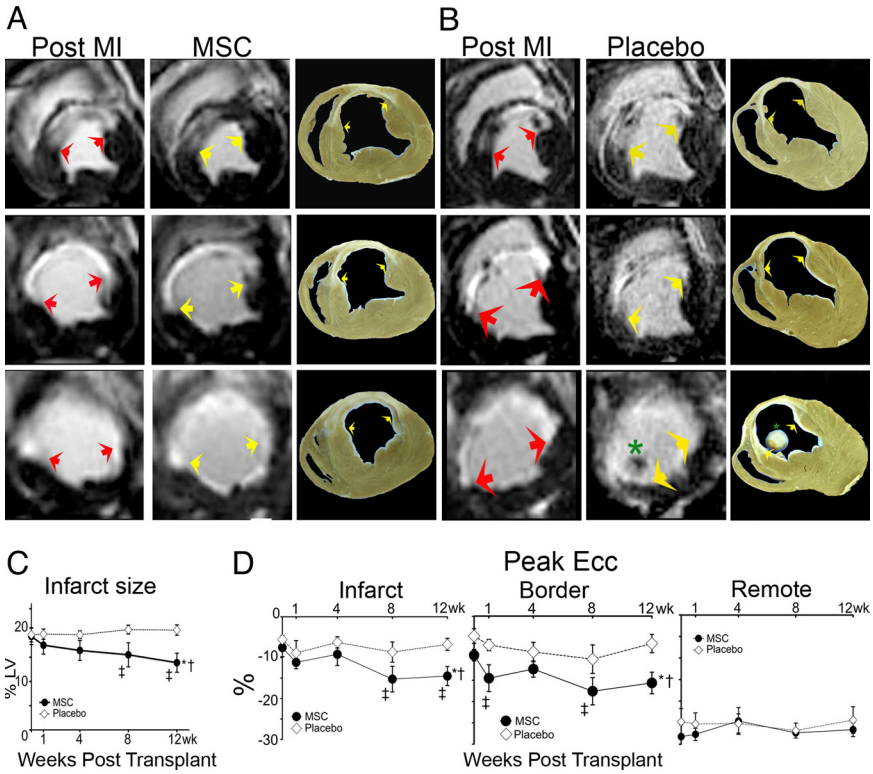

Fig. 4. Infarct size assessment and regional myocardial function. (*A* and *B*) Sequential short axis heart sections from base (top) to apex (bottom) of delayed gadolinium enhancement MRI images depicting the infarct extension (white) before treatment and 12 weeks following MSC therapy (*A*) compared with the placebo (*B*). Comparable gross pathology sections are shown adjacent to the MRI images. Arrows delineate the infarct extension, and the asterisk illustrates the presence of a thrombus near the apex in a placebo animal. (*C*) Reduction in infarct size following 8 and 12 weeks post MSC transplantation versus placebo (*$P <$ 0.001 within MSC group ANOVA, $^{\dagger}P < 0.05$ between groups ANOVA, $^{\ddagger}P < 0.001$ vs. preinjection status by Student-Newman-Keuls test). (*D*) Myocardial strain analysis represented by peak Ecc decreased in response to MSC-treatment in infarct (*Left*) and border (*Center*) areas but remained constant in the remote uninfarcted zone (*Right*) (*$P < 0.05$ for ANOVA within MSC group, $^{\dagger}P < 0.05$ ANOVA between groups, $^{\ddagger}P < 0.05$ vs. preinjection status by Student-Newman-Keuls test). At least five MRI time points were analyzed for MSC-treated hearts ($n = 6$) and placebo-treated hearts ($n = 4$). For week-4 tagged MRI images and week-8 delayed contrast enhancement MRI analysis, MSCs ($n = 4$) and placebo ($n = 4$).

group while the MSC group had significant thickening ($P < 0.05$; Table 1).

Regional LV Function. To determine contractile capacity of the regenerated myocardium, tagged MRI images were used to calculate peak Eulerian circumferential shortening (Ecc) in the infarct, border, and remote zones. As shown (Fig. 4*D*), at 12 weeks after MI, all animals had decreased function in the infarct (peak Ecc $-6.7 \pm 1.4\%$) and border ($-7.3 \pm 1.2\%$) zones, compared with a normal negative Ecc in the remote non-infarct zone ($-26.9 \pm 2.0\%$). Regional contractile function showed significant improvement over the post cell injection period in the both border and infarct zones of MSC-treated animals (Fig. 4*D* *Left* and *Center*). In contrast, contractile function exhibited further declines in placebo-treated animals (Fig. 4*D*).

Myocardial Perfusion. First-pass perfusion MRI was used to assess the impact of MSCs on myocardial blood flow. The average myocardial upslope of the time-attenuation curves normalized to the maximum LV blood pool attenuation density was used as a measure of tissue perfusion (23). At week 12, all animals had diminished flow in infarct (0.13 ± 0.01) and border (0.14 ± 0.01) zones as compared to the remote zone (0.26 ± 0.01; $P < 0.001$). Twelve weeks after therapy, the decrease in basal flow persisted in placebo-treated animals. In contrast, beginning at week 4 following cell delivery, the basal flow increased in the MSC-treated group ($P < 0.001$ by ANOVA; Fig. 5*A* and Fig. S5 *a* and *b*).

Global LV Function. The decrease in infarct size together with increased contractility and perfusion resulted in improved global LV function. Whereas ejection fraction remained constant in placebo, it increased significantly in the MSC-treated group ($P <$ 0.05 by ANOVA; Fig. 5*B*).

In an attempt to further elucidate the mechanisms of the functional changes that occurred, the correlations between decrease in infarct size, increase in contractility, and increase in perfusion in the border zone were all calculated. All parameters strongly correlated (Fig. 5 *C–E*). Most importantly, cell engraftment in the peri-infarct area correlated with the increase in regional LV function ($R = 0.85$), decrease in infarct size ($R = -0.67$), and myocardial perfusion ($R = 0.76$; Fig. 5 *F–H*). Interestingly, the number of Y^{pos} vessels also correlated with the increase in myocardial blood flow ($R = 0.86$) and the reduction in infarct size ($R = -0.74$; Fig. S5).

Discussion

Here we demonstrate the ability of bone marrow-derived adult MSCs to integrate into the chronically injured heart. Heretofore, the ability of MSCs to adopt cardiac phenotypes in vivo has been highly controversial, leading to the interpretation that functional benefits of these cells derive largely from paracrine mechanisms (9–13, 19). Our results demonstrate the presence of viable MSCs in infarct and border zones 12 weeks after transplantation into a chronic ischemic scar. The MSCs differentiate into cardiomyocytes and blood vessel elements that integrate into host myocardium, form gap junctions, and contribute to the restoration of

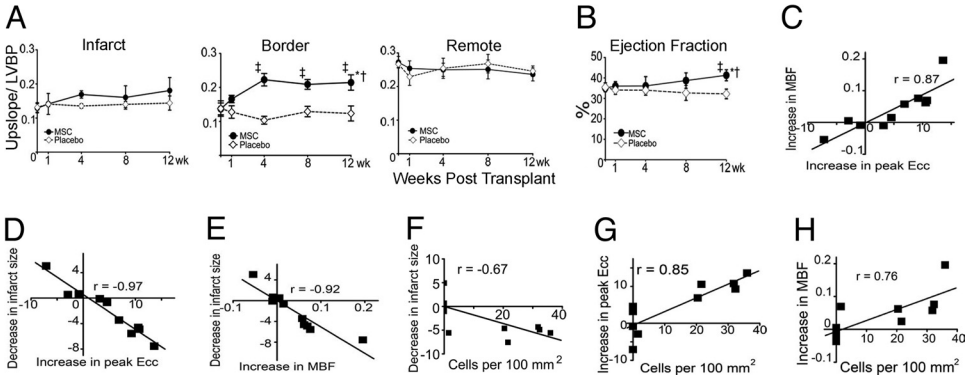

Fig. 5. Myocardial blood flow and segmental contractility showed improvement related to the cell engraftment. (*A*) Quantitative analysis of first-pass perfusion MRI in the infarct (*Left*), border (*Center*), and remote (*Right*) myocardium demonstrating the improvement in the MSC-treated group compared to placebo group (*$P < 0.05$ for ANOVA within MSC, †$P < 0.001$ ANOVA between groups, ‡$P < 0.05$ vs. preinjection status by Student-Newman-Keuls test; LVBP, left ventricular blood pool). (*B*) LV ejection fraction improves in MSC group at 12 weeks posttransplantation (*$P < 0.05$ for ANOVA within MSC, †$P < 0.05$ ANOVA between groups, ‡$P < 0.05$ vs. preinjection status by Student-Newman-Keuls). (*C–H*) The functional outcomes in heart function (i.e., infarct size reduction, increase in contractility and increase in tissue perfusion) showed related interaction between them (*C–E*) and with the magnitude of cells detected (*F–H*) at 12 weeks after injection ($P <$ 0.05 for all Pearson correlations). At least five time points for first-pass perfusion MRI image analysis. MSCs-treated hearts ($n = 6$) and placebo ($n = 4$) hearts for most of the time points except at 4 weeks for ejection fraction ($n = 8$, 4 MSC and 4 placebo).

cardiac function and tissue perfusion. These findings document the ability of an adult bone marrow-derived stem cell to engraft and differentiate into cardiac cellular elements and, as such, have important therapeutic implications (7, 8, 24).

The present findings offer detailed phenotypic and mechanistic insights into the actions of MSCs to repair chronically ischemic myocardium. Our model recapitulates the phenotype of ischemic cardiomyopathy with antero-apical transmural scar and infarct expansion. Even in the face of the substantial cardiac remodeling evident in our model, injection of MSCs clearly led to infarct size reduction and reverse remodeling. Thus, even late injection of cells into the postinfarct heart has a desirable phenotypic outcome. Our results provide comprehensive documentation that the MSCs engraft, differentiate into myocytes, engender neovascularization, and maintain reservoirs of immature cells. As we have previously reported in an acute MI model, the area of greatest engraftment and regeneration resides in the border zone between infarcted tissue and viable myocardium. In addition, as we and others have previously reported (23, 25, 26), increased tissue perfusion is the earliest observable outcome of cell therapy in the early post infarct heart, an effect that occurs here as well. Infarct size reduction and enhanced global and regional function are progressive effects that occur time dependently over a 3-month period. Our findings do not exclude the many other important properties ascribed to MSCs, including extracellular matrix remodeling (11), progenitor cells recruitment (27), and release of paracrine factors (13). Indeed, it is this constellation of features that likely accounts for the ability of MSCs to engraft in the chronically scarred heart and to stimulate not only functional recovery but also reverse remodeling.

Many studies have failed to document MSC differentiation into cardiac cell constituents in the infarcted heart (12, 28, 29). A significant number of these studies relied solely on green fluorescent protein (GFP) to track cell fate following transplantation, its continued presence being necessary as a marker of engraftment. Given that GFP labeling can diminish and that the transgene construct might be silenced as cells proliferate and differentiate, detection of differentiation could be obscured (30, 31). Conversely, in cases where multiple cell tagging techniques (fluorescent dyes, nanoparticles, sex mistmatch) were used, strong evidence of engraftment and cardiomyocyte formation has been shown (6, 24).

Other recent work has challenged the in vivo immunoprivileged state of MSCs, asserting that they exert a delayed host response 2 weeks posttransplantation (32, 33). A graft-versus-host immunologic response, once triggered, would dramatically impair heart function in allogeneic cell-treated subjects. In contrast, we observed improvement of the previously deteriorated cardiac muscle function. Supporting our approach, there are an extensive number of studies employing MSCs in a broad spectrum of hematological and nonmalignant diseases to attenuate the immune response, therefore, modulating the recipient environment (34, 35).

Due to limitations associated with the long-term cell tracking, we could not assess the extent to which MSCs are lost immediately postdelivery or during the follow-up period. Interestingly, we observed a large number of transplanted cells that remained undifferentiated and persisted in the interstitial compartment. Our findings are in agreement with previous work that reveals a spectrum of maturity of newly transplanted cells. In this regard, Boni and Rota et al. reported that Lin^{neg} $c\text{-}kit^{pos}$ cardiac precursor cells resulted in small bands of regeneration composed of myocytes of different size as well as highly proliferative clusters of committed progenitor cells in rodent hearts (36, 37). The role of the smaller, undifferentiated cells requires further investigation, but it is attractive to speculate that they may form a reservoir for ongoing tissue homeostasis, niche reconstitution, or paracrine factor production (38, 39). Future work will be required to fully assess the nature of these cells and whether they retain immature stem cell characteristics.

In vivo modalities to track this cellular kinetics immediately following transplantation remains a challenge in large animal models. We used MRI to sequentially compare the treated and untreated areas. While overall estimation of ejection fraction can underestimate the functional improvement (22), we used both global and segmental wall analysis for contractility and perfusion to characterize precise changes (40–42). Indeed, changes were present in tissue perfusion, as well as global and regional function, and cell engraftment correlated with regional function in the border zone of the infarct. This finding is highly biologically plausible, as the border zone is the site of greatest activity for cell engraftment and differentiation.

The present report corroborates the survival and renewal of MSCs in the chronic ischemic myocardium and its contribution to improve the cardiovascular physiology after MI. The chal-

lenge to rebuild an established myocardial scar with cell-based therapy is highly desirable and fulfills a crucial unmet clinical need. These findings strongly support the clinical development of this strategy to treat chronic ischemic heart failure.

Materials and Methods

Closed-chest MI induction by occlusion of the mid-left anterior descending artery with subsequent reperfusion was performed in female swines. Twelve weeks later, allogeneic male MSCs or placebo were injected in the infarct and border zone. New myocardium and vessel formation were assessed by double immunofluorescence and FISH analysis. Evaluation of myocardial contractile function was performed by cardiac MRI. For additional information, see *SI Materials and Methods*.

ACKNOWLEDGMENTS. This work was supported by National Heart, Lung, and Blood Institute Grants U54-HL081028 (Specialized Center for Cell-Based Therapy) and R01-HL084275.

1. Chien KR, Domian IJ, Parker KK (2008) Cardiogenesis and the complex biology of regenerative cardiovascular medicine. *Science* 322:1494–1497.
2. Assmus B, et al. (2006) Transcoronary transplantation of progenitor cells after myocardial infarction. *N Engl J Med* 355:1222–1232.
3. Meyer GP, et al. (2006) Intracoronary bone marrow cell transfer after myocardial infarction: Eighteen months' follow-up data from the randomized, controlled BOOST (bone marrow transfer to enhance ST-elevation infarct regeneration) trial. *Circulation* 113:1287–1294.
4. Psaltis PJ, Zannettino AC, Worthley SG, Gronthos S (2008) Concise review: Mesenchymal stromal cells: Potential for cardiovascular repair. *Stem Cells* 26:2201–2210.
5. Belema-Bedada F, Uchida S, Martire A, Kostin S, Braun T (2008) Efficient homing of multipotent adult mesenchymal stem cells depends on FROUNT-mediated clustering of CCR2. *Cell Stem Cell* 2:566–575.
6. Reinecke H, Minami E, Zhu WZ, Laflamme MA (2008) Cardiogenic differentiation and transdifferentiation of progenitor cells. *Circ Res* 103:1058–1071.
7. Orlic D, et al. (2001) Bone marrow cells regenerate infarcted myocardium. *Nature* 410:701–705.
8. Beltrami AP, et al. (2003) Adult cardiac stem cells are multipotent and support myocardial regeneration. *Cell* 114:763–776.
9. Murry CE, et al. (2004) Haematopoietic stem cells do not transdifferentiate into cardiac myocytes in myocardial infarcts. *Nature* 428:664–668.
10. Balsam LB, et al. (2004) Haematopoietic stem cells adopt mature haematopoietic fates in ischaemic myocardium. *Nature* 428:668–673.
11. Uemura R, Xu M, Ahmad N, Ashraf M (2006) Bone marrow stem cells prevent left ventricular remodeling of ischemic heart through paracrine signaling. *Circ Res* 98:1414–1421.
12. Gnecchi M, et al. (2005) Paracrine action accounts for marked protection of ischemic heart by Akt-modified mesenchymal stem cells. *Nat Med* 11:367–368.
13. Gnecchi M, Zhang Z, Ni A, Dzau VJ (2008) Paracrine mechanisms in adult stem cell signaling and therapy. *Circ Res* 103:1204–1219.
14. Pittenger MF, et al. (1999) Multilineage potential of adult human mesenchymal stem cells. *Science* 284:143–147.
15. Aggarwal S, Pittenger MF (2005) Human mesenchymal stem cells modulate allogeneic immune cell responses. *Blood* 105:1815–1822.
16. Hare JM, Chaparro SV (2008) Cardiac regeneration and stem cell therapy. *Curr Opin Organ Transplant* 13:536–542.
17. Toma C, Pittenger MF, Cahill KS, Byrne BJ, Kessler PD (2002) Human mesenchymal stem cells differentiate to a cardiomyocyte phenotype in the adult murine heart. *Circulation* 105:93–98.
18. Pijnappels DA, et al. (2008) Forced alignment of mesenchymal stem cells undergoing cardiomyogenic differentiation affects functional integration with cardiomyocyte cultures. *Circ Res* 103:167–176.
19. Mangi AA, et al. (2003) Mesenchymal stem cells modified with Akt prevent remodeling and restore performance of infarcted hearts. *Nat Med* 9:1195–1201.
20. Noiseux N, et al. (2006) Mesenchymal stem cells overexpressing Akt dramatically repair infarcted myocardium and improve cardiac function despite infrequent cellular fusion or differentiation. *Mol Ther* 14:840–850.
21. Rose RA, et al. (2008) Bone marrow-derived mesenchymal stromal cells express cardiac-specific markers, retain the stromal phenotype, and do not become functional cardiomyocytes in vitro. *Stem Cells* 26:2884–2892.
22. Carr CA, et al. (2008) Bone marrow-derived stromal cells home to and remain in the infarcted rat heart but fail to improve function: an in vivo cine-MRI study. *Am J Physiol Heart Circ Physiol* 295:H533–H542.
23. Schuleri KH, et al. (2008) Early improvement in cardiac tissue perfusion due to mesenchymal stem cells. *Am J Physiol Heart Circ Physiol* 294:H2002–H2011.
24. Rota M, et al. (2007) Bone marrow cells adopt the cardiomyogenic fate in vivo. *Proc Natl Acad Sci USA* 104:17783–17788.
25. Tillmanns J, et al. (2008) Formation of large coronary arteries by cardiac progenitor cells. *Proc Natl Acad Sci USA* 105:1668–1673.
26. Halkos ME, et al. (2008) Intravenous infusion of mesenchymal stem cells enhances regional perfusion and improves ventricular function in a porcine model of myocardial infarction. *Basic Res Cardiol* 103:525–536.
27. Shabbir A, Zisa D, Suzuki G, Lee T (2009) Heart failure therapy mediated by the trophic activities of bone marrow mesenchymal stem cells: A noninvasive therapeutic regimen. *Am J Physiol Heart Circ Physiol* 296:H1888–H1897.
28. Nygren JM, et al. (2004) Bone marrow-derived hematopoietic cells generate cardiomyocytes at a low frequency through cell fusion, but not transdifferentiation. *Nat Med* 10:494–501.
29. Terada N, et al. (2002) Bone marrow cells adopt the phenotype of other cells by spontaneous cell fusion. *Nature* 416:542–545.
30. Toth ZE, et al. (2007) Sensitive detection of GFP utilizing tyramide signal amplification to overcome gene silencing. *Exp Cell Res* 313:1943–1950.
31. Brazelton TR, Blau HM (2005) Optimizing techniques for tracking transplanted stem cells in vivo. *Stem Cells* 23:1251–1265.
32. Nauta AJ, et al. (2006) Donor-derived mesenchymal stem cells are immunogenic in an allogeneic host and stimulate donor graft rejection in a nonmyeloablative setting. *Blood* 108:2114–2120.
33. Poncelet AJ, Vercruysse J, Saliez A, Gianello P (2007) Although pig allogeneic mesenchymal stem cells are not immunogenic in vitro, intracardiac injection elicits an immune response in vivo. *Transplantation* 83:783–790.
34. Symons HJ, Fuchs EJ (2008) Hematopoietic SCT from partially HLA-mismatched (HLA-haploidentical) related donors. *Bone Marrow Transplant* 42:365–377.
35. Burt RK, et al. (2008) Clinical applications of blood-derived and marrow-derived stem cells for nonmalignant diseases. *JAMA* 299:925–936.
36. Rota M, et al. (2008) Local activation or implantation of cardiac progenitor cells rescues scarred infarcted myocardium improving cardiac function. *Circ Res* 103:107–116.
37. Boni A, et al. (2008) Notch1 regulates the fate of cardiac progenitor cells. *Proc Natl Acad Sci USA* 105:15529–15534.
38. Mazhari R, Hare JM (2007) Mechanisms of action of mesenchymal stem cells in cardiac repair: Potential influences on the cardiac stem cell niche. *Nat Clin Pract Cardiovasc Med* 4(Suppl 1):S21–S26.
39. da Silva ML, Caplan AI, Nardi NB (2008) In search of the in vivo identity of mesenchymal stem cells. *Stem Cells* 26:2287–2299.
40. Amado LC, et al. (2006) Multimodality noninvasive imaging demonstrates in vivo cardiac regeneration after mesenchymal stem cell therapy. *J Am Coll Cardiol* 48:2116–2124.
41. Carlsson M, Osman NF, Ursell PC, Martin AJ, Saeed M (2008) Quantitative MR measurements of regional and global left ventricular function and strain after intramyocardial transfer of VM202 into infarcted swine myocardium. *Am J Physiol Heart Circ Physiol* 295:H522–H532.
42. Amado LC, et al. (2005) Cardiac repair with intra-myocardial injection of allogeneic mesenchymal stem cells following myocardial infarction. *Proc Natl Acad Sci USA* 102:11474–11479.